Chromophore Relaxation in a Side-Chain Methacrylate Copolymer Functionalized with 4-[N-Ethyl-N-(2-hydroxyethyl)]ammo-2′-chloro-4′- nitroazobenzene

ARTICLE *in* MACROMOLECULES · FEBRUARY 2004

Impact Factor: 5.8 · DOI: 10.1021/ma035714j

Chromophore Relaxation in a Side-Chain Methacrylate Copolymer Functionalized with 4-[*N*-Ethyl-*N*-(2-hydroxyethyl)]amino-2′-chloro-4′-nitroazobenzene

P. A. Ribeiro,*,‡ D. T. Balogh,† José L. C. Fonseca,§ and J. A. Giacometti⊥

Instituto de Física de São Carlos, Universidade de São Paulo, CP 369, 13560-970 São Carlos, SP, Brazil; CEFITEC-Centro de Física e Investigação Tecnológica, Departamento de Física, Faculdade de Ciências e Tecnologia, Universidade Nova de Lisboa, 2829-516 Caparica, Portugal; Departamento de Química, Universidade Federal do Rio Grande do Norte, Campus Universitário, Lagoa Nova, CP 1662, 59072-970, Natal, RN, Brazil; and Faculdade de Ciência e Tecnologia, Universidade Estadual Paulista, 19060-900, Presidente Prudente, SP, Brazil

Received November 14, 2003; Revised Manuscript Received January 23, 2004

ABSTRACT: A side-chain methacrylate copolymer functionalized with the nonlinear optical chromophore 4-[*N*-ethyl-*N*-(2-hydroxyethyl)]amino-2′-chloro-4′-nitroazobenzene, disperse red-13, was prepared and characterized. The chromophore relaxation was investigated measuring the decay of the electrooptic coefficient r_{13} and the complex dielectric constant at different temperatures. Results obtained below and above T_g were analyzed using the Kohlrausch−Williams−Watts (KWW) equation, through the study of the temperature dependence of the KWW parameters. Above T_g the relaxation time experimental data were fitted to the Williams−Landel−Ferry (WLF) equation and its parameters determined. Chromophore relaxation leading to the decrease of electrooptic properties was found associated with a primary α relaxation. The obtained WLF equation parameters were introduced into the Adam−Gibbs−Tool−Narayanaswamy−Moynihan equation, and the overall relaxation time temperature dependence was successfully obtained in terms of the fictive temperature, accounting for the sample thermal treatment and allowing optimized thermal treatment to be found. The copolymer KWW stretching parameter at the glass transition temperature lies close to the limit value for short-range interactions, i.e., 0.6, suggesting that the chromophore group is participating in primary α relaxation.

I. Introduction

The most common polymeric materials with nonlinear optical (NLO) properties are the side-chain polymers, which are synthesized by covalently linking organic NLO chromophore molecules to a given polymeric backbone.[1] The azobenzene chromophore group confers to polymers their NLO features and also the reversible cis−trans photoisomerization, leading to optical switching, optical storage, and surface relief grating formation.[2] For second-order NLO optical processes, such as second-harmonic generation and the linear electrooptic effect (Pockel's effect), polymers must be submitted to the electric poling in order to generate polar orientation of the chromophore. Poling is usually performed either applying a bias voltage[3] to the sample or charging it in a corona triode.[4,5] The orientational order of chromophores that results is usually unstable, and a strong effort has been made to investigate relaxation processes of such NLO chromophores in order to obtain more stable polymeric materials. The electric polarization is a measure of such orientational order, and it is related to the linear electrooptic and second-harmonic generation effects.

Several relaxation models have been attempted for NLO polymers. In fact, the decay of the electrooptic coefficient can be fitted with different functions such as biexponential,[6] Kohlrausch−Williams−Watts stretched exponential (KWW),[7,8] single-exponential plus KWW, van der Vorst,[9] and Dissado−Hill power laws.[10,11] The KWW decay function is given by:

$$\Phi(t) = \exp\left[-\left(\frac{t}{\tau}\right)^{b}\right] \tag{1}$$

Usually such an equation provides a good data fitting and meaningful parameters τ and b, τ representing a characteristic relaxation time and b the exponential stretching. The KWW equation was initially considered an empirical function, found to fit most of the experimental relaxation data, with no particular meaning for the b parameter. However, physical meaning can be achieved if one takes into account that the KWW equation is the solution for the Brownian motion of a particle interacting with randomly distributed traps or sinks.[12,13] Under this model a defined microscopic meaning for the b parameter can also be inferred. Thus, dependences of τ and b on temperature are of great relevance to understand the microscopic behavior of polymers and also to predict the final NLO properties of the glassy state, obtained when cooling the material from the liquid state. Regarding phenomenological viscoelasticity, if $b = 1$, the relaxation process corresponds to a single relaxation time. For $b < 1$, the relaxation process is associated with a relaxation time distribution, that is, a relaxation spectrum centered at the characteristic relaxation time τ. The lower the value of b is, the broader the relaxation spectrum will be. Tobolsky et al. have shown that an increase in molecular weight implies a decrease in b,[14] and Monteiro et al.

† Universidade de São Paulo.
‡ Universidade Nova de Lisboa.
§ Universidade Federal do Rio Grande do Norte.
⊥ Universidade Estadual Paulista.
* To whom correspondence should be addressed: Fax +351 21 294 85 49; e-mail pfr@fct.unl.pt.

10.1021/ma035714j CCC: $27.50
Published on Web 02/27/2004

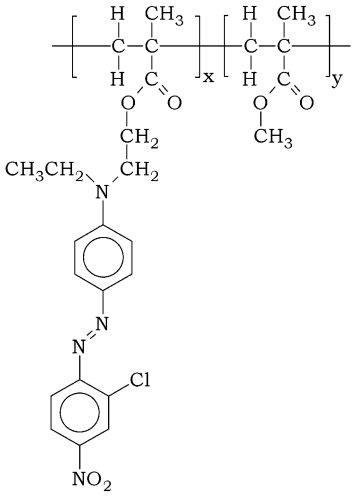

Figure 1. Chemical structure of the random MMA−DR13 copolymer. *X* and *Y* values determine the percentage of each monomer.

associated the decrease in *b* with the increase in phase segregation in polyurethanes.[15] In other words, anything that makes the relaxation process more heterogeneous such as higher polydispersity or higher molecular weight implies in more possibilities of entanglements between the polymer chains and will contribute to a decrease of *b* and to the relaxation spectrum broadening.

In the present work, the preparation and characterization of the side-chain methyl methacrylate, MMA-DR13, an acrylic copolymer functionalized with different percentages of the chromophore disperse red-13, 4-[*N*-ethyl-*N*-(2-hydroxyethyl)]amino-2′-chloro-4-nitroazobenzene, DR13, are briefly described. A detailed study of the relaxation of chromophore orientation was performed by monitoring the electrooptic coefficient decay, in time domain, below the glass transition temperature, T_g. Above T_g, dielectric spectroscopy measurements were used, as the electrooptic decay was too fast to be measured. Electrooptic coefficient decay and dielectric spectroscopy results were analyzed using the KWW function, from which the dependences of τ and *b* on temperature were determined. The temperature dependence of the relaxation time was calculated from dielectric data above T_g, and the obtained values were fitted to the Williams−Landel−Ferry (WLF) equation.[16] The relaxation time values below T_g, obtained from electrooptic measurements, were predicted by introducing WLF constants into the modified Adams−Gibbs (AG) equation, which accounts for the glass transition kinetics.[17]

The article is organized as follows. Section II gives the experimental results of the copolymer preparation and its characterization, corona poling, and measurement techniques. Section III shows the results of the relaxation measurements, and section IV presents the discussion and conclusions.

II. Experimental Section

The random copolymer, MMA-DR13, shown in Figure 1, was prepared from solution copolymerization of methyl methacrylate (MMA, Aldrich) and 4-[*N*-ethyl-*N*-(2-methacryloxyethyl)]-amino-2′-chloro-4′-nitroazobenzene (DR13MA). The DR13MA monomer was synthesized by the esterification of the commercial dye 4-[*N*-ethyl-*N*-(2-hydroxyethyl)]amino-2′-chloro-4′-nitroazobenzene (DR13, Aldrich) with methacryloyl chloride.[18] The copolymerization of DR13MA and MMA monomers was performed using methyl ethyl ketone as solvent and 2,2′-azobis(butyronitrile) (AIBN) as initiator, at reflux temperature for 9 h. The resultant copolymer was precipitated, exhaustively washed with methanol, and dried in a vacuum desiccator for about 72 h. Different ratios of DR13MA and methyl methacrylate monomers were used to prepare copolymers with chromophore weight ratios of 9 and 43 wt %, being designated as MMA-DR13(9 wt %) and MMA-DR13(43 wt %), respectively. Small quantities of MMA-DR13(4 wt %) were also prepared to be used as trial samples. Copolymers were characterized by UV−vis in DMF solution, using a Hitachi U2001 spectrophotometer, and by FTIR, samples in KBr pellets, using a BOMEM DA-8 spectrophotometer. Thermal behavior of the samples was characterized by differential scanning calorimetry (DSC), using a TA calorimeter model 2910 (ambient to 250 °C, 20 °C/min and under N_2), and thermogravimetry mass loss (TGA), using a Shymadzu Twi50 thermal analyzer (ambient to 700 °C, 10 °C/min and under N_2).

Number-average (M_n) and by weight-average (M_w) molecular weights, as well the polydispersivity, were obtained by size exclusion chromatography (SEC) (THF as eluent and polystyrene standards). It was found that values of M_n were ca. 23 000 and 18 000 g/mol for the MMA-DR13(9 wt %) and MMA-DR13-(43 wt %), respectively, while values of M_w were 40 000 and 35 000. Thus, polydispersities are of the order of 1.7 and 1.9, respectively. Thin-layer chromatography (silica gel using dichloromethane/*n*-hexane 70/30) confirmed the absence of nonreacted monomers.

All copolymers in DMF solution showed a maximum optical absorption at 505 nm. Copolymer films showed a blue shift of 15 nm compared to the solution spectra, probably due to aggregation of the chromophores in the film, similarly to Langmuir−Blodgett films.[18] The main IR absorption bands of MMA were present: 2960, 2850 cm^{-1} (C−H stretching), 1732 cm^{-1} (C−O stretching of ester groups), 1242, 1252, and 1134 cm^{-1} (asymmetric and symmetric C(=O)−O and O−C−C stretching vibrations of ester group). Regarding DR13MA-related absorptions, the following bands are present in the spectra of all copolymers: 1599 and 1500 cm^{-1} (C=C stretching in benzene rings), 1518 cm^{-1} (NO_2 asymmetric stretching), and 1336 cm^{-1} (NO_2 symmetric stretching).

Films with thickness of about 10 μm were cast from chloroform copolymer solutions (0.5−2% w/w). All solutions were filtered with a syringe Millipore Durapore 0.45 μm filter. Substrates such as optical crown type glass, glass covered with indium tin oxide (ITO), or aluminum plates were employed. Samples were dried for 30 min at room conditions and then submitted to a primary vacuum at 130 °C for 24 h for solvent removal.

To achieve the second-order NLO properties, i.e., to orient the side-chain chromophore dipolar groups, a corona triode setup was used.[4,5] Such a technique has been preferred to pole NLO polymers because it offers better radial uniformity polarization on sample[4] and a good control of final surface potential, and the metallic grid gives protection against surface attack from corona species, which are known to deteriorate polymer surfaces.[4,19,20] The corona triode consisted of a sharp point, a stainless steel grid with a stainless steel mesh of wires of 0.1 mm diameter, and a metallic sample holder.[4] The corona triode was mounted inside an oven, allowing the temperature to be controlled. A voltage was applied to the grid, and a high-voltage supply (±20 kV, operating as a constant current source) was used to generate the corona discharge. A corona current of ±5 μA was used in the experiments. The electric contact between the sample holder and the conductive ITO layer was obtained using silver paint. Such a procedure avoids the interference of the glass slide on the poling conditions. The sample was heated to the temperature of 120 °C, a grid voltage ranging from 400 to 600 V was applied, and the corona discharge turned on. Poling was performed for 30 min; subsequently, the sample was cooled to room temperature, with the corona discharge on, at a rate of about 10 °C/min. The poling process terminated at room temperature, and power supplies turned off. The above experimental conditions yielded maximum electrooptic activity in samples as reported elsewhere[4] in a detailed study.

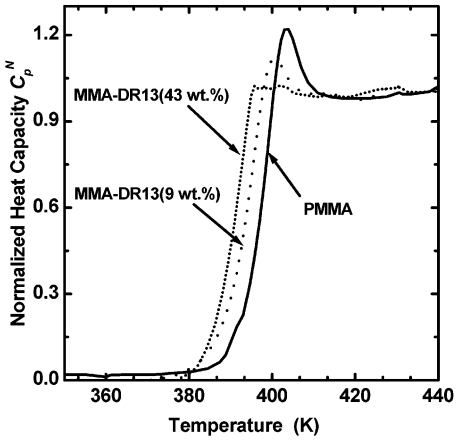

Figure 2. Normalized heat capacity C_P^N curves obtained from differential scanning calorimetry thermograms for MMA−D13(9 wt %) and MMA−DR13(43 wt %) copolymers and PMMA.

A scanning Mach-Zhender interferometer was used to measure the electrooptic coefficient, r_{13}, of the poled MMA−DR13 copolymer. The experimental setup is similar to the one described by Singer et al.[21] In these measurements, films deposited onto ITO glass substrates were used. The bare surface of the film was metallized with an ∼10 nm aluminum layer by thermal evaporation in a vacuum, which is practically transparent to the 10 mW, He−Ne, 633 nm laser beam used in the electrooptic coefficient measurements. The light was linearly polarized, and the laser beam of diameter 2 mm impinged the sample at a right angle with respect to its surface. The electrooptic effect was produced in the samples by applying a modulation sinusoidal voltage to the aluminum electrode by means of a soft metallic spring to avoid mechanical stress. Interference fringes were scanned by applying a ramp voltage to a piezoelectric driven mirror. Measurement conditions were the following: modulation frequency of 2 kHz, frequency of fringe displacement within a range from 0.01 to 0.05 s^{-1}, and fringe visibility better than 60%.

The dielectric permittivity measurements were performed with a Solartron 1260 impedance analyzer in the frequency range from 1 Hz to 1 MHz, applying a 0.3 V sine voltage. For these measurements MMA-DR13 films were casted onto 1 mm aluminum circular plates, the upper electrode being a 200 nm aluminum layer deposited by vacuum thermal evaporation.

Note that temperature values are given in degrees Celsius, but in equations and in graphs their correspondig values on the Kelvin scale were used.

III. Results

3.1. Copolymer Thermal Characterization. DSC thermograms were obtained for some copolymers with different MMADR13 monomer contents (9 and 43 wt %), the normalized heat capacity, C_P^N, being calculated using the following expression:[22]

$$C_P^N = \frac{C_P(T) - C_{PL}(T)}{C_{PH}(T) - C_{PL}(T)} \qquad (2)$$

where C_P is the experimental value and C_{PH} and C_{PL} are the values of C_P obtained by extrapolation at high- and low-temperature limits, i.e., far from T_g. Curves of Figure 2 show that T_g values, taken at $C_P^N \cong 0.5$, are around 118 °C, decreasing slightly as chromophore content is increased. For comparison, it is also shown the corresponding curve of poly(methyl methacrylate), PMMA, sample (M_w = 350 000). In the data analysis, to be shown in section IV, a T_g value of 118 °C was employed for all copolymers.

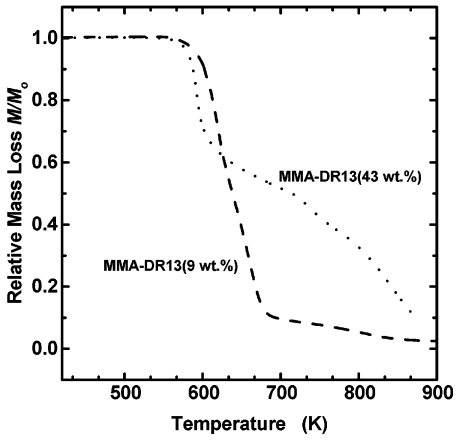

Figure 3. Thermogravimetric loss mass curves for MMA−DR13(9 wt %) and MMA−DR13(43 wt %) copolymers.

TGA loss mass measurements, shown in Figure 3, indicated that thermal degradation of the samples started around 327 °C, much higher than the temperatures used in this work. Thus, no degradation of the copolymer is expected to occur during measurements. In addition, the copolymer MMA−DR13(43 wt %) showed a decomposition curve with a different pattern, as compared to one of MMA−DR13(9 wt %). A possible explanation is that the highly conjugated chromophores could produce the cross-linking of the macromolecule chains with the action of temperature, resulting in systems that would be more difficult to decompose. As a consequence, the residual mass at the end of TGA curves are higher for higher chromophore contents.

3.2. Isothermal Electrooptic Decay. Under optimized corona poling conditions[4] the maximum values of r_{13} achieved, for MMA−DR13 samples with chromophore contents of 9 and 43 wt %, were 3 and 8 pm/V, respectively. For the sake of clearness, normalized values of r_{13} with respect to the initial ones will be shown.

Decay curves of normalized electrooptic coefficient, r_{13}, at different temperatures are shown in parts a and b of Figure 4 respectively for the MMA−DR13(9 wt %) and MMA−DR13(43 wt %) samples. These curves reveal that the decay increases with temperature and also that it is more accentuated for the MMA−DR13(43 wt %) sample.

The decay curves were best fitted to the KWW equation. Other decay functions such as the exponential, biexponential, biexponential plus KWW, or van der Vorst did not allow good fitting as obtained with the KWW function (results not shown here). As a consequence, the KWW function was used to analyze the relaxation data. This procedure is usually applied with success in the literature for NLO polymers.[4,23,24] The fitting curves are shown in Figure 4a,b by the full lines.

3.3. Dielectric Relaxation. It is worth mentioning that measurements of r_{13} could be performed only below T_g because its decay at higher temperatures is too fast to be accurately measured using the Mach−Zender interferometer. An alternative procedure to probe the chromophore relaxation is from the dielectric response in the frequency domain. The complex dielectric permittivity $\epsilon^* = \epsilon' + j\epsilon''$ is related to the KWW decay function $\Phi(t)$, eq 1, by the Laplace transform as:[8]

$$\frac{\epsilon^*(\omega) - \epsilon(\infty)}{\epsilon(0) - \epsilon(\infty)} = -\int_0^\infty \exp(-j\omega t)\left(\frac{d\Phi(t)}{dt}\right) dt \qquad (3)$$

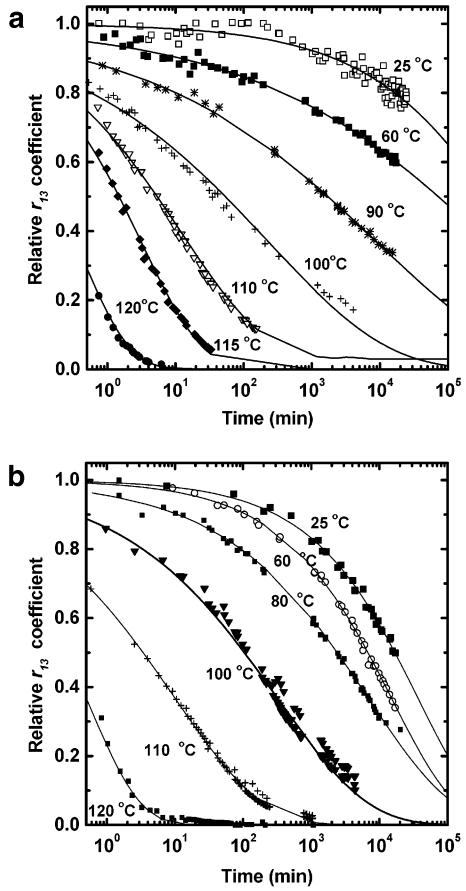

Figure 4. (a) Experimental results for electrooptic decay (points) and KWW fitting curves for MMA−DR13(9 wt %) sample. Temperatures of measurements are indicated in each curve. (b) Experimental results for electrooptic decay (points) and KWW fitting curves for MMA−DR13(43 wt %) sample. Temperatures of measurements are indicated in each curve.

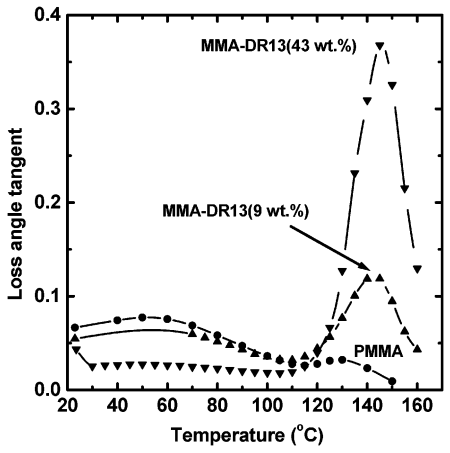

Figure 5. Loss angle tangent data vs temperature taken at the frequency of 100 Hz, for MMA−DR13(9 wt %), MMA−DR13(43 wt %), and PMMA samples. The lines are guide lines.

where $\epsilon(0)$ and $\epsilon(\infty)$ are the real parts of low- and high-frequency limits of the dielectric permittivity, respectively. Determination of τ and b KWW function parameters using eq 3 is not a straightforward process since the analytical evaluation of the integral of Laplace transform is not possible for all values of b. In this work, the approximations outlined by Weiss et al.[25] were used.

The tan $\delta = \epsilon''/\epsilon'$ vs temperature curves, obtained at 100 Hz, are shown in Figure 5. Two relaxation peaks were observed; the lower one, around 60 °C, is associated with a β relaxation and the higher one, around 140 °C, with an α relaxation. The curve of PMMA (Aldrich, M_w = 350 000) is also included for comparison. (Only the β peak is observable at the frequency of 100 Hz in the temperature range displayed in the figure.) The β peak, corresponding to MMA−DR13 samples, should be attributed to the hindered rotation of the ester (−$COOCH_3$) group of the MMA.[26] In the case of MMA−DR13(43 wt %) samples, it is believed that the β peak does not occur because of the higher volume that this bulky chromophore group occupies, making more hindered the chain rotation. The amplitude of the α peak is highly dependent on the chromophore content. Thus, it seems that the chromophore side-group relaxation follows the α relaxation. This behavior is somehow expected in side-chain NLO polymers rather than in guest−host since the chromophore molecules are bound to the copolymer backbone so that its orientational relaxation should be linked to the primary α relaxation.

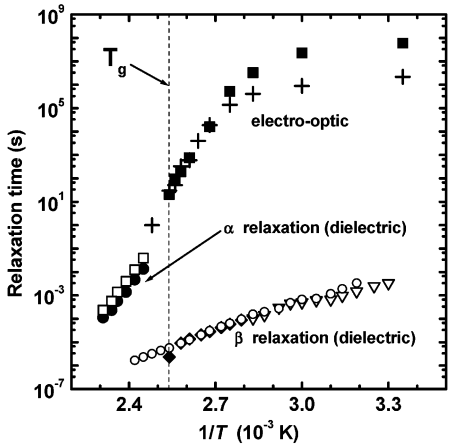

Figure 6. Relaxation times vs the inverse of the absolute temperature. Data represented by solid square and cross symbols were obtained from electrooptic coefficient measurements respectively for MMA−DR13(9%) and MMA−DR13-(43%) samples. Solid circle and open square symbols correspond to α relaxation data obtained from dielectric measurements respectively for MMA−DR13(9%) and MMA−DR13-(43%) samples. Finally, open circle, solid diamond, and open down triangle symbols correspond to β relaxation data obtained from dielectric measurements respectively for MMA−DR13(4%), MMA−DR13(9%), and MMA−DR13(43%) samples.

3.4. Temperature Dependence of Parameters. Figure 6 shows a plot of the KWW relaxation time, τ, versus the reciprocal of temperature. The data were obtained from the fitting of the r_{13} decay curves and also from the tan δ curves employing the Weiss procedure;[25] τ values for both α and β peaks were found. It is worth mentioning two points: first, τ values corresponding to the β relaxation peaks are much smaller in comparison to the corresponding ones for the α relaxation and also of those determined from the electrooptic decay; second, τ values obtained from r_{13} decay, below T_g, and from α peaks, above T_g, seem to lie along the same curve. From this result one may conclude that the r_{13} decay and the tan δ peak arises from the same relaxation processes; i.e., they are associated with the dipolar chromophore disordering, the α relaxation process in the copolymer. Furthermore, the $\tau(T)$ vs $1/T$ dependence for the α relaxation (Figure 6) clearly shows a deviation from Arrhenius behavior at high temperatures, indicating the fragile character[12,27] of MMA−DR13 glass former.

Results for the dependence of KWW b parameter on temperature, not shown here, reveal small changes in

the investigated temperature range. From nearly constant at low temperatures it presents a small increase near T_g and stabilizes at higher temperatures. Generally speaking, one can say that, for both compositions, 98% of the values fall into the interval 0.50 ± 0.06, and the value of b at T_g is in the interval 0.55 ± 0.05. The meaning for these values will be discussed in the next section. It should be pointed out that the shape of the electrooptic decay curves of Figure 4 is dependent on the sample particular aging process. As a consequence, the τ and b parameters obtained from the fit of these data to KWW equation will be also dependent on aging, in such a way that these parameters are seen to increase as one goes from fast cooling to slow cooling from T_g. Typically, for a decay at 60 °C, τ can increase up to 1 order of magnitude as one goes from cooling at a rate of about 20 °C/min to about 0.2 °C/min, while b increases up to 1.5 times in the same conditions. However, a general equation accounting for the $\tau(T)$ dependence in terms of the aging process can be found from the dielectric relaxation data obtained above T_g, as will be seen in the next section.

IV. Discussions and Conclusions

Before discussing the results, it is worthwhile to review here the approach usually employed to interpret the dependence of $\tau(T)$ on T. It is known that $\tau(T)$ is well accounted for by the WLF equation[28] within a temperature range from T_g to (T_g + 100 °C) while the Arrhenius equation[16] is suitable below T_g. More general equations were obtained by Addam−Gibbs[17] (AG), when interpreting the relaxation process as the cooperative interaction due the packing of polymer segments as the temperature is decreased from above the glass transition, and by Tool−Narayanaswamy−Moynihan (TNM)[29−33] as a result of considering enthalpy relaxation in terms of a fictive temperature, T_f, as a measure of departure from thermal equilibrium and accounting for the glass transition kinetic behavior. These concepts were reexamined by Hodge and Berens,[34] resulting in the following equation, the Addam−Gibbs−Tool−Narayanaswamy−Moynihan (AG-TNM) equation, for the relaxation time temperature dependence:

$$\frac{\tau(T)}{\tau_g} = \exp\left[-\frac{B}{T_g - T_0} + \frac{B}{T\left(1 - \frac{T_0}{T_f(T)}\right)}\right] \qquad (4)$$

where τ_g is the relaxation time measured at T_g, B is an activation temperature, BR, with R the universal gas constant, being an activation energy per mole, and T_0 is the temperature at which the configurational entropy would be zero. For a process of a glass formation during a cooling process, at a constant cooling rate q from a temperature T_i above T_g, the fictive temperature can be determined by the following equation:[34]

$$T_f(T) = T_i + \int_{T_i}^{T} dT' \left\{1 - \exp\left[-\left(\frac{1}{q}\int_{T'}^{T}\frac{dT''}{\tau(T)}\right)^b\right]\right\} \qquad (5)$$

$\tau(T)$ and b are the usual parameters in the KWW equation, and $T'$and T'' are the integration variables. Determination of $T_f(T)$ requires a cumbersome procedure since b, $\tau(T)$, and the cooling/heating dynamics should be known in all temperature ranges. To circumvent such a difficulty, the $\tau(T)$ dependence is habitually analyzed in two limit cases, since the exponential of eq 4 contains both the high- and the low-temperature behaviors of the WLF and Arrhenius equations, as follows:

(a) Limit Case−Above T_g. At the limit of high temperatures one has $T_f \approx T$, and eq 4 becomes:

$$\frac{\tau(T)}{\tau_g} = \exp\left[-\frac{B}{T_g - T_0} + \frac{B}{T - T_0}\right] \qquad (6)$$

which is the Vogel−Fulcher−Tammann−Hesse[35−37] (VFTH) equation. It shows the same dependence of the WLF equation, given by:

$$\log\left(\frac{\tau(T)}{\tau_g}\right) = -C_1^g + \frac{C_1^g C_2^g}{T - T_0} \qquad (7)$$

where C_1^g and C_2^g are constants. According to the free volume theory[26] $C_1^g = b'/2.303f(T_g)$ and $C_2^g = f(T_g)/\alpha_f(T_g)$, where b' is a polymer dependent constant, $f(T_g)$ is the free volume fraction, and $\alpha(T_g)$ is the volumetric expansion coefficient both at T_g. It should be noted that as eq 7 is the logarithm form of eq 6, then $B = 2.303C_1^gC_2^g$ and $T_0 = T_g - C_2^g$.[38]

(b) Limit Case−Below T_g. At the low-temperature limit, the fictive temperature tends to a constant value, $T_f = T_f'$, and eq 4 becomes:

$$\frac{\tau(T)}{\tau_g} \propto \exp\left[-\frac{B}{T\left(\frac{T_0}{T_f'} - 1\right)}\right] \qquad (8)$$

which has the same form as the Arrhenius equation.

Since the WLF behavior usually occurs above T_g,[27] one can infer that the C_1^g and C_2^g WLF parameters can be used in the AG-TNM equation. Such a parametrization has been successfully applied to polyimides functionalized with similar size NLO azo chromophres and allowed a complete relaxation description over more than 15 orders of magnitude in time.[39]

The fitting parameters of the experimental data, using the WLF equation (eq 7) for MMA−DR13(9 wt %) and MMA−DR13(43 wt %) copolymers, are displayed in Table 1. Results revealed that for both compositions the C_1^g parameters are basically the same and the C_2^g fall in the same range. Similar values of C_1^g means that a unique relaxation curve can be obtained if the relaxation time is plotted normalized to T_g. In fact, eq 8 predicts this behavior if the final fictive temperature is set equal to T_g. In this case, one obtains:[40]

$$\log\frac{\tau(T)}{\tau_g} = C_1^g\frac{T_g - T}{T} \qquad (9)$$

and normalization with respect to $(T_g - T)/T$ arises.

The fitting curves obtained using the Arrhenius and VFTH functions are shown in Figure 7 by dashed and full lines, respectively, plotted as a function of $(T_g - T)/T$. It should be noticed that eq 5 is expected to account

Table 1. Values of WLF Equation Parameters C_1^g, C_2^g, and T_0 Obtained from Fitting the Experimental Normalized Relaxation Times above T_g

MMA−DR13 (wt %)	C_1^g	C_2^g (K)	T_0 (K)
9	12 ± 2	40 ± 10	350 ± 20
43	12 ± 2	50 ± 10	340 ± 20

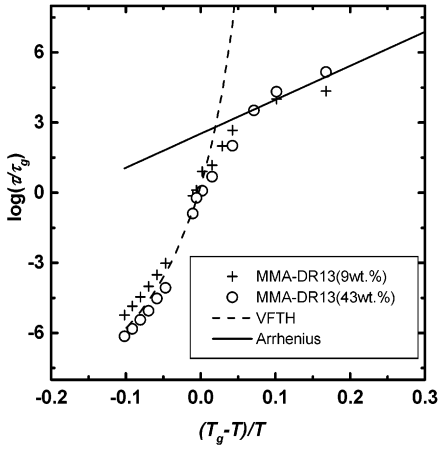

Figure 7. Plot of relaxation times (normalized to τ_g) as a function of the parameter $(T_g - T)/T$, for both MMA−DR13-(9%) and MMA−DR13(43%) samples, and fitting curves to WLF and Arrhenius equations.

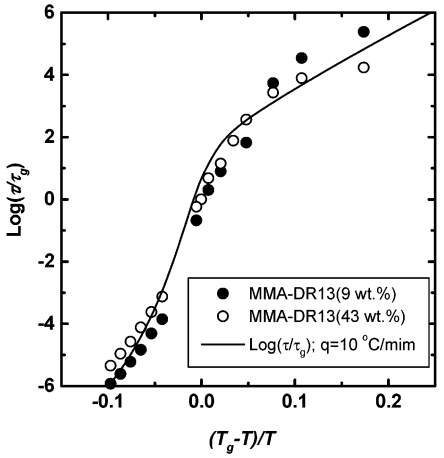

Figure 8. Result from fitting of experimental data to the AG-TNM equation for both MMA−DR13(9%) and MMA−DR13-(43%) samples.

for the kinetics of the glass formation for a particular cooling process, in such a way that when introduced into eq 8 one expects to fit the experimental data in the region near T_g. This is shown by the full line in Figure 8, which is the curve obtained with the AG-TNM equation using C_1^g and C_2^g parameters listed in Table 1, a cooling rate of 10 °C/min, and the KWW *b* parameter equal to 0.5, which is the average value in the temperature range used in the experiments. Fitting results indicate that a good prediction of the orientational stability of NLO chromophores in MMA−DR13 copolymers can be achieved.

The orientational stability can be better understood using eq 8, as the *B* parameter is related to the Arrhenius activation energy, E_a, of the primary α relaxation, responsible for randomization of the chromophore orientation. The expression for E_α in terms of the final fictive temperature T_f' follows from eq 8:

$$E_a(T) = \frac{2.303 C_1^g C_2^g}{1 - \frac{T_0}{T_f'}} \qquad (10)$$

To finish this point, the analysis performed above is used to predict the thermal treatment process that leads to the lowest final fictive temperature T_f' as close as possible to the T_0 value. In Figure 9 the fictive temperature dependence on the cooling rate for MMA−DR13-(43 wt %), calculated from eq 5, using $b = 0.5$, is shown. As one can expect, the lower the cooling rate is, the lower the final fictive temperature is, and a more stable glass can be obtained. Low cooling rate requires a long time exposure of the sample to the corona discharge, leading to the surface sample deterioration. Previous results obtained for the MMA−DR13 copolymers indicated that the exposure of the sample to the corona discharge should not exceed much more than 60 min to minimize sample damage.[4] Consequently, cooling rates smaller than 2 °C/min should be avoided, as the exposure will exceeds the maximum allowed. Indeed, at a cooling rate of 2 °C/min, the cooling process will take about 45 min, which seems to be fine. However, further thermal stability of the copolymer can be achieved if one includes an annealing step during the cooling process at a given rate. The main concern here is to find the optimum annealing temperature for a given time interval, compatible with the advisable for maximum corona exposure of about 60 min. For this purpose the final fictive temperature has been calculated at chosen cooling rate for different annealing temperatures and times. The calculation follows from eq 5, which has to be modified to include an annealing step.[39] The plot of final fictive temperatures as a function of the annealing temperature is shown in

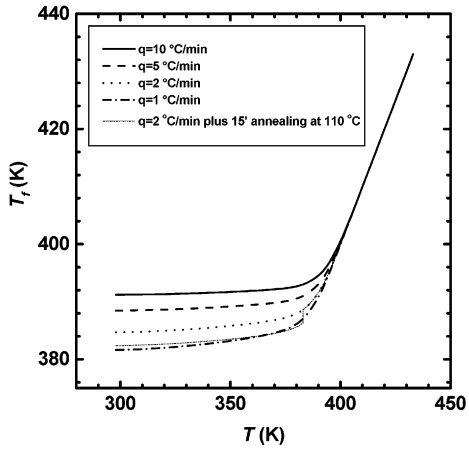

Figure 9. Fictive temperature, T_f, temperature dependence, for different thermal treatments.

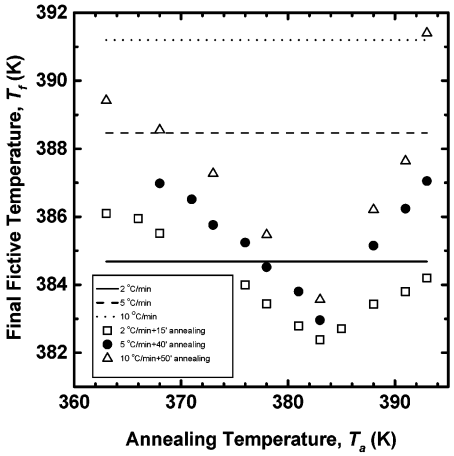

Figure 10. Final fictive temperature, T_f', vs annealing temperature, T_a, for several annealing times and cooling rates. The horizontal lines indicate the final fictive temperatures achieved for the cooling rates of 2, 5, and 10 °C/min.

Figure 10. The curves show a minimum around 110 °C, indicating that this value is the ideal one to perform the annealing. The lowest final fictive temperature is reached for a cooling rate of 2 °C/min and annealing at 110 °C for 15 min. The T_f' value in this case is 109 °C, lower than that one achieved when cooling at 2 °C/min and close to the one achieved when cooling at 1 °C/min (Figure 9). The total time of exposure to the corona discharge process will be in this case of 65 min, which guarantees minor sample surface damage.

As a measure of the fragile characteristic of MMA−DR13, revealed in the plot of Figure 6, one can estimate the fragility index, defined in terms of the WLF equation as:[41]

$$m_{\mathrm{WLF}} = \left[\frac{\partial(\log(\tau/\tau_g))}{\partial(T_g/T)}\right]_{T=T_g} \tag{11}$$

which according to eq 9 gives:

$$m_{\mathrm{WLF}} = \frac{C_1^g}{C_2^g} T_g \tag{12}$$

From this equation, considering the values of C_1^g and C_2^g in Table 1 and those of T_g, one obtain the fragility indexes of 120 ± 50 and 90 ± 40 for MMA−DR13(43 wt %) and MMA−DR13(9 wt %), respectively. The large values confirm the fragile MMA−DR13 glass former is. The replacement of the (−$COOCH_3$) group by the chromophore group in the side chain seems confer a less fragile behavior since the index is lower than that of PMMA, which is 145.[41]

The fragility of the glass former has been correlated with the KWW stretching *b* parameter.[41] The general trend is that a glass former presenting large values of *b* tend to present fragile behavior, i.e., a small fragility index. In this way one may expect larger values of *b* parameter for MMA−DR13 than that obtained for PMMA, although both polymeric systems have similar glass transition temperatures. The values of *b* at the glass transition temperature are claimed to be dominated by the numbers 0.43 and 0.6 respectively associated with long-range Coulombic interactions and short-range interactions.[13] As a consequence, the expected values for long-chain polymeric systems would be of 0.43, accounting for long-range Coulombic intrachain interactions associated with the backbone relaxation. However, exceptions are known for polymeric chains having side groups that somehow actively participate in the relaxation process. Normally, side groups are known to increase the interchain interactions since they act as spacers or even add rotational mode to the interchain interaction.[13] In this situation $b(T_g)$ is expected to be closer to the short-range forces limit, i.e., 0.6. This seems to be the case for MMA−DR13 copolymer with $b(T_g)$ of 0.55 ± 0.05. This effect should indeed be remarkable in MMA−DR13, since in PMMA $b(T_g)$ falls in opposite side with a value of 0.34.[41] This result is consistent with a strong contribution of the chromophore group for the primary α relaxation.

Acknowledgment. The authors thank FAPESP, CAPES, and CNPq, Brazil, and Fundação Ciência e Tecnologia−PRAXIS XXI, Portugal, for financial support and to A. C. Hernandez for gently supplying high-quality electrooptic calibration crystals and to S. C. Zilio and F. D. Nunes for the help with electrooptic experimental setup.

References and Notes

(1) Marks, T. J.; Ratner, M. A. *Angew. Chem., Int. Ed. Engl.* **1995**, *34*, 155−173.
(2) Mendonça, C. R.; Dhanabalan, A.; Balogh, D. T.; Misoguti, L.; dos Santos, D. S., Jr.; Pereira da Silva, M. A.; Giacometti, J. A.; Zílio, S. C.; Oliveira, O. N., Jr. *Macromolecules* **1999**, *32*, 1493−1499.
(3) Singer, K. D.; Sohn, J. E.; Lalama, S. J. *Appl. Phys. Lett.* **1986**, *49*, 248−250.
(4) Ribeiro, P. A.; Balog, D. T.; Giacometti, J. A. *IEEE Trans. Dielect. El. In.* **2000**, *7*, 572−577.
(5) Giacometti, J. A.; Oliveira, O. N., Jr. *IEEE Trans. Elec. Insul.* **1992**, *27*, 924−943.
(6) Hampsch, H. L.; Yang, J.; Wong, G. K. J.; Torkelson, J. M. *Macromolecules* **1990**, *23*, 3640−3654.
(7) Kohlraush, R. *Ann. Phys. Chem.* **1854**, *91*, 179.
(8) Williams, G.; Watts, D. C. *Trans. Faraday Soc.* **1970**, *66*, 80.
(9) van der Vorst, M. C. P. J.; van Cassel, R. A. P. *Macromol. Symp.* **1995**, *90*, 47.
(10) Dissado, L. A.; Hill, D. H. *Nature (London)* **1979**, *279*, 685.
(11) Dureiko, R. D.; Schuele, D. E.; Singer, K. D. *J. Opt. Soc. Am. B* **1998**, *15*, 338−350.
(12) Privalko, V. P. *J. Non-Cryst. Solids* **1999**, *255*, 259−263.
(13) Philips, J. C. *Rep. Prog. Phys.* **1996**, *59*, 1133.
(14) Knoff, W. F.; Hopkins, I. L.; Tobolsky, A. V. *Macromolecules* **1971**, *4*, 750−754.
(15) Monteiro, E. E. C.; Fonseca, J. L. C. *J. Appl. Polym. Sci.* **1997**, *65*, 2227−2236.
(16) Williams, M. L.; Landel, R. F.; Ferry, J. D. *J. Am. Chem. Soc.* **1955**, *77*, 3701.
(17) Ferry, J. D. In *Viscoelastic Properties of Polymers*, 3rd ed.; Wiley: New York, 1980.
(18) Dhanabalan, A.; Balogh, D. T.; Riul, A., Jr.; Giacometti, J. A.; Oliveira, O. N., Jr. *Thin Solid Films* **1998**, *323*, 257−264.
(19) Haridoss, S.; Perlman, M. M. *J. Appl. Phys.* **1984**, *55*, 1332−1338.
(20) Raposo, M.; Ribeiro, P. A.; Marat Mendes, J. N. *Ferroelectrics* **1992**, *34*, 235−240.
(21) Singer, K. D.; Lalama, S. L.; Sohn, J. E.; Small, R. D. In *Nonlinear Properties of Organic Molecules and Crystals*; Chemla, D. S., Zyss, E. J., Eds.; Academic Press: New York, 1987; Vol. II, Chapter 81, p 444.
(22) Moynihan, C. T.; Eastel, A. J.; DeBolt, M. A.; Tucker, J. *J. Am. Ceram. Soc.* **1976**, *59*, 12.
(23) Goodson, T., III; Wang, C. H. *Macromolecules* **1993**, *26*, 1837−1840.
(24) Dhinojwala, A.; Wong, G. K.; Torkelson, J. M. *Macromolecules* **1993**, *26*, 5943−5953.
(25) Weiss, G. H.; Bendler, J. T.; Dishon, M. *J. Chem. Phys.* **1985**, *83*, 1424−1427.
(26) McCrum, N. G.; Read, B. E.; Williams, G. In *Anelastic and Dielectric Relaxation in Polymeric Solids*; Wiley: London, 1967.
(27) Vilgis, T. A. *Phys. Rev. B* **1993**, *47*, 2882−2885.
(28) Williams, M. L.; Landel, R. F.; Ferry, J. D. *J. Am. Chem. Soc.* **1955**, *77*, 3701.
(29) Toll, A. Q.; Eichlin, C. G. *J. Am. Ceram. Soc.* **1931**, *14*, 276.
(30) Toll, A. Q. *J. Am. Ceram. Soc.* **1946**, *29*, 240.
(31) Toll, A. Q. *J. Am. Ceram. Soc.* **1948**, *31*, 177.
(32) Narayanaswamy, O. S. *J. Am. Ceram. Soc.* **1971**, *54*, 491.
(33) Moynihan, C. T.; Easteal, A. J.; Debolt, M. A.; Tucker, J. *J. Am. Ceram. Soc.* **1976**, *59*, 12−16.
(34) Hodge, I. M.; Berens, A. R. *Macromolecules* **1982**, *15*, 762−770.
(35) Vogel, H. *Phys. Z.* **1921**, *22*, 645.
(36) Tammann, G.; Hesse, W. Z. *Anorg. Allg. Chem.* **1926**, *156*, 245.
(37) Fulcher, G. S. *J. Am. Ceram. Soc.* **1925**, *8*, 339.
(38) Angell, C. A. *Polymer* **1997**, *38*, 6261−6266.
(39) Kaatz, P.; Prêtre, P.; Meier, U.; Stalder, U.; Bosshard, C.; Günter, P.; Zysset, B.; Stähelin, M.; Ahlheim, M.; Lehr, F. *Macromolecules* **1996**, *29*, 1666−1678.
(40) Prêtre, P.; Kaatz, P.; Bohren, A.; Günter, P.; Zysset, B.; Ahlheim, M.; Stähelin, M.; Lehr, F. *Macromolecules* **1994**, *27*, 5476−5486.
(41) Böhmer, R.; Ngai, K. L.; Angell, C. A.; Plazek, D. J. *J. Chem. Phys.* **1993**, *99*, 4201−4209.

MA035714J